Ultra-broadband highly efficient mode converter at 1 μm fabricated by a line-focused CO_2 laser

Xin Tian (田 鑫)[1,2,3], Hao Li (李 昊)[1,2,3], Le Liu (刘 乐)[1,2,3], Meng Wang (王 蒙)[1,2,3], Xiaoming Xi (奚小明)[1,2,3], and Zefeng Wang (王泽锋)[1,2,3,*]

[1]*College of Advanced Interdisciplinary Studies, National University of Defense Technology, Changsha 410073, China*

[2]*State Key Laboratory of Pulsed Power Laser Technology, Changsha 410073, China*

[3]*Hunan Provincial Key Laboratory of High Energy Laser Technology, Changsha 410073, China*

*Corresponding author: zefengwang_nudt@163.com

Received May 17, 2019; accepted August 22, 2019; posted online November 26, 2019

We report here an ultra-broadband linearly polarized (LP) LP_{01}–LP_{11} mode converter operating at 1 μm based on a long period fiber grating (LPFG) fabricated in a conventional two-mode fiber (TMF) by a line-focused CO_2 laser. The measured 3 dB bandwidth is about 240 nm, which is the broadest bandwidth for such fiber mode converters. The maximum conversion efficiency between the LP_{01} and LP_{11} modes is >99% over the range of 1000 nm to 1085 nm, almost covering the whole emission band of Yb^{3+}, which is useful for further power scaling of high-power fiber lasers operating at the 1 μm band.

OCIS codes: 060.2340, 060.3735, 060.2330, 140.3510.

doi: 10.3788/COL201917.120602.

With the rapid development of fiber communication, a typical single-mode fiber (SMF) has reached the limit of transmission capacity, and several new techniques have emerged to enlarge information capacity. Mode-division multiplexing (MDM), which has been widely used in fiber communication networks, is a promising technology for increasing the transmission capacity of optical fibers[1,2]. A mode converter, especially in communication systems, is an essential component of MDM and can realize the conversion between the fundamental mode and high-order modes. A variety of techniques have been reported to achieve mode conversion. For example, the photonic lantern[3–5] and fiber Bragg grating (FBG)[6,7] have attracted increasing attention because of the advantages of lower insertion loss, higher coupling efficiency, and easier fabrication. Long period fiber gratings (LPFGs), which have been widely used in fiber communication, fiber sensors, and fiber amplifiers for the advantage of no background scattering, also can be applied to generate mode conversion between the fundamental mode and high-order modes[8–10].

In 2002, Ramachandran *et al.* reported the LPFG written in a few-mode fiber (FMF) using UV laser irradiation and analyzed the spectrum properties of the LPFG-based mode converter[11,12]. Unlike the conventional LPFGs, the power coupling of the LPFG-based mode converter takes place between two co-propagating core modes in the fiber. Many reports emerged about the mode converter based on the LPFG fabricated by UV laser exposure[11], CO_2 laser point-by-point writing technique[13,14], coiled fiber[15], electromagnetic inducing[16], and so on. In 2016, Zhao *et al.* presented an LPFG and a titled LPFG fabricated by a CO_2 laser, generating two orthogonal vector modes ($HE_{21,odd}$ and $HE_{21,even}$) by adjusting the input polarization states[13].

In 2018, Zhao *et al.* realized mode conversions between linearly polarized mode LP_{01} and LP_{11}, LP_{21}[14]. In addition, mode conversion from LP_{01} to LP_{11} can be realized by writing a pair of superimposed LPFGs (SLPFGs)[17] and a mode-selective coupler[18]. Conversion efficiency of LPFGs can be up to 99%[19].

At present, the Yb-doped large-mode-area double-cladding fiber is still the first choice for high-power fiber lasers. However, for power scaling, conventional fundamental mode oscillation in the cavity is limited due to the high-energy density and nonlinear effects of fused silica. Previous reports have proved that high-order modes propagation during the gain process is one of the best ways to overcome the problems mentioned above[20,21]. As an important all-fiber mode converting device, LPFGs can be employed in high-order fiber lasers to obtain a higher gain or mitigation of the nonlinear effects[20,21], such as stimulated Raman scattering (SRS) and stimulated Brillouin scattering (SBS). However, up to now, nearly all studies of LPFGs are focused on the 1.5 μm band.

Here, we report an ultra-broadband mode converter based on an LPFG at 1 μm inscribed with a line-focused CO_2 laser. An optical spectrum analyzer (OSA) and a beam profile analyzer are used to on-line monitor the fabrication process. By optimizing the grating parameters, a record 3 dB bandwidth of about 240 nm for such devices is obtained, and the maximum conversion efficiency between the LP_{01} and LP_{11} modes is higher than 99% over the range of 1000 nm to 1085 nm, which covers the main operating band of current high-power fiber lasers. We believe that this ultra-broadband mode converter is useful for the power scaling in 1 μm high-power laser systems.

In an LPFG-based mode converter, the mode coupling process takes place between two core modes, i.e., LP_{01} and LP_{11}, when the phase matching condition is satisfied.

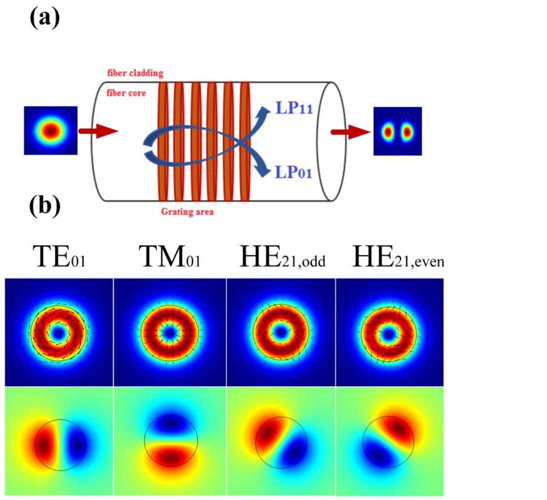

Fig. 1. (a) Mode coupling scheme of an LPFG mode converter. (b) The density profile of the LP_{11} mode and four high-order vector beams (TE_{01}, TM_{01}, $HE_{21,\mathrm{even}}$, $HE_{21,\mathrm{odd}}$) at 1064 nm, and their x component of electric-field simulations with the standard step index fiber of SMF-28e (the core and cladding diameters are ~8.2 μm and 125 μm, the refractive indices of the core and cladding are 1.4689 and 1.4630 at 1064 nm) by the finite element method.

Figure 1(a) shows a schematic of the coupling between the guided modes in the core. According to the coupled-mode theory, the phase matching condition can be written as

$$\lambda_{\mathrm{res}} = (n_{\mathrm{eff}}^{\mathrm{LP}_{01}} - n_{\mathrm{eff}}^{\mathrm{LP}_{11}})\Lambda, \tag{1}$$

where λ_{res} is the resonant wavelength, $n_{\mathrm{eff}}^{\mathrm{LP}_{01}}$ and $n_{\mathrm{eff}}^{\mathrm{LP}_{11}}$ are the effective indices of LP_{01} and LP_{11}, respectively, and Λ is the period of the LPFG. The mode conversion efficiency can be calculated with mode coupling equations

$$\frac{\partial A_{01}}{\partial z} = i\beta_{01}A_{01} + i\kappa_{12}A_{11}, \frac{\partial A_{11}}{\partial z} = i\beta_{11}A_{11} + i\kappa_{22}A_{01}, \tag{2}$$

where A_{01} and A_{11} are the amplitude of the modes LP_{01} and LP_{11}; κ_{12} and κ_{22} represent the cross-coupling coefficient. When the phase matching condition is satisfied, the power of the fundamental mode will be converted gradually to the LP_{11} mode, and the conversion efficiency is determined by the coupling length z and the index modulation.

In a weakly guiding fiber, the real existing modes are degenerated, which is called an LP mode and is formed by the overlap of several high-order modes, which share the same density profile and a nearly identical effective index. For example, the degenerated mode LP_{11} is the overlap of four high-order modes TE_{01}, TM_{01}, $HE_{01,\mathrm{odd}}$, and $HE_{01,\mathrm{even}}$, and the density profile is shown in Fig. 1(b). The upper part of the picture is the electric energy density time average of different degenerated modes; the bottom is the x component of the electric field with the four modes. However, these high-order modes have different effective refractive indices when the fiber has a high numerical aperture (NA), and they can maintain their polarization during propagation.

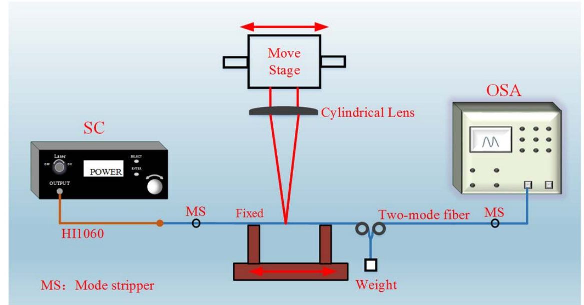

Fig. 2. Fabrication setup: SC, supercontinuum light source; OSA, optical spectrum analyzer; PC, polarization controller.

The fabrication system for LPFG mode converters based on SMF-28e is shown in Fig. 2. A continuous-wave CO_2 laser (Synrad, wavelength at 10.6 μm) is used. During the fabrication process, in order to simplify the laser beam control and increase the fabrication efficiency, the CO_2 laser irradiation is focused into a line using a cylindrical lens and periodically moved along the fiber axis point-by-point, which will induce asymmetrical refractive index changes in the two orthogonal directions and form an LPFG-based mode converter. The period is controlled by moving the stage, and the refractive index modulation is controlled with the power and exposure time of the CO_2 laser. The mode conversion efficiency spectrum measurement setup consists of a supercontinuum light source (NKT, Super compact, 450–2400 nm), an OSA, and a pair of mode strippers (MSs). The first MS is used to make sure that only the fundamental mode propagates before the mode converter, and the second MS is used to strip off the high-order modes generated by the mode convertor. A weight is employed to keep horizontal when the fiber is heated. During the fabrication process, the fundamental mode transmission spectrum will be monitored by the OSA, and the mode conversion efficiency can be calculated.

To achieve high conversion efficiency, it is important to obtain proper grating parameters, including period, length, and refractive index modulation. To verify the effective refractive indices of the two modes, an FBG is inscribed in the fiber with a UV exposure technique. The measured transmission spectrum of the FBG is shown in Fig. 3. Two resonant wavelengths at 1061.44 nm and 1059.804 nm correspond to the core modes LP_{01} and LP_{11}, respectively. The difference of effective indices between the two modes can be calculated from the central wavelength of the two modes and the period of the FBG. By calculating the parameters we measured, the period of the LPFG satisfying the resonant wavelength of 1064 nm is about 425 μm. The excitation ratio of the LP_{11} mode is extremely weak because of our no-offset splicing. So, the coupling between forward LP_{01} and backward LP_{11} is also very weak, and the corresponding resonant wavelength is not obvious in the transmission.

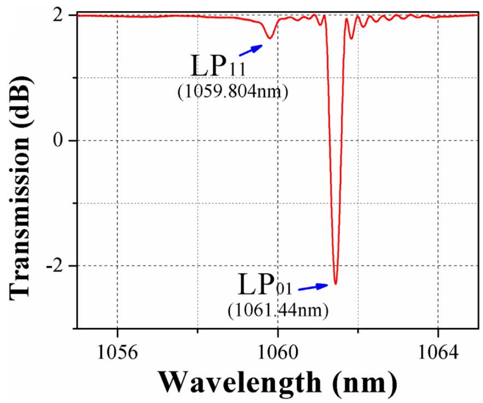

Fig. 3. Transmission spectrum of the FBG for experiments.

We simulate the phase matching condition at different wavelengths for fiber of SMF-28e, and the phase matching curve (PMC) at the 1 μm band is shown in Fig. 4(a). The cutoff wavelength of the fundamental mode is ~1260 nm, which means SMF-28e is a TMF (supporting LP_{01} and LP_{11}) at 1 μm. The relationship between the period and wavelength (also meaning PMC) is achieved by calculating the refractive indices of the LP_{01} and LP_{11} modes in a range of wavelength according to Eq. (1). As shown in Fig. 4(a), there is a turning-around point (TAP) near 1050 nm. The PMC reveals that for a certain grating period, the phase matching condition can be satisfied at two different wavelengths. It means that the coupling at these two wavelengths is strong and dual-peaks will be shown in the conversion spectrum. The small interval of the dual-peaks results in a superposition of the two peaks and a broadband mode conversion.

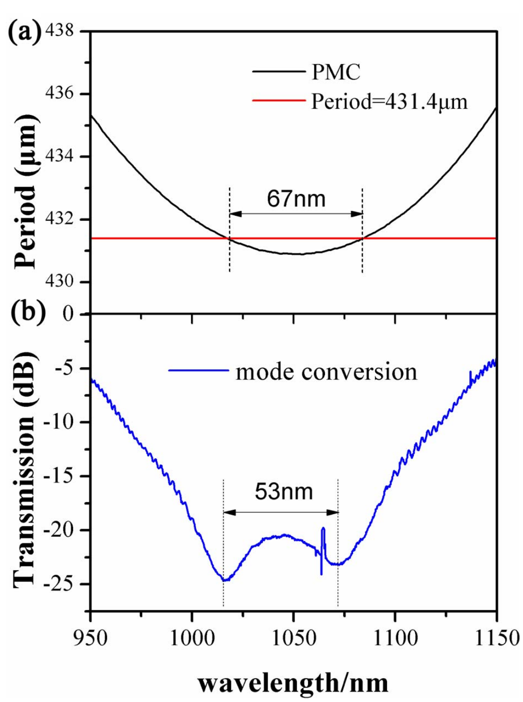

Fig. 4. (a) Simulation PMC of the fiber of SMF-28e; (b) the measured transmission spectrum of the mode converter.

To optimize the parameters of the mode converter, lots of measurements have been done. The optimized parameters of the grating are 423 μm of the period, 17 periods (7.191 mm of the grating length), 7.4 W and 300 ms of the laser power and exposure time for seven scanning cycles [these parameters of the laser introduce a minimum damage to the fiber and give a negligible background transmission loss, which can be verified in Fig. 5(a)]. The measured transmission spectrum of the mode converter, given by subtracting the transmission spectra before and after the mode converter is inscribed in fiber SMF-28e in Fig. 2, is shown in Fig. 4(b). There are two attenuation peaks in the transmission spectrum, corresponding to two phase matching points. The measured interval of the two peaks is about 53 nm, which is close to the simulation results. A broadband transmission dip can be observed around 1060 nm, and the depth of the transmission dip is about 25 dB, corresponding to the conversion efficiency of >99%. The 20 dB bandwidth is about 80 nm and the 3 dB bandwidth is about 240 nm [shown in Fig. 5(a)], which is the broadest bandwidth for such fiber mode converters. This is due to the small difference in dispersion between LP_{01} and LP_{11} modes[11,22,23]. The small peak in the spectrum at 1064 nm is related to the pump source of the supercontinuum.

The fabricated mode converter is then characterized with a measurement setup shown in Fig. 6. A CCD camera and a single frequency light source at 1064 nm are used to monitor the change of the mode patterns. The output light of the mode converter is collimated, and a CCD camera is

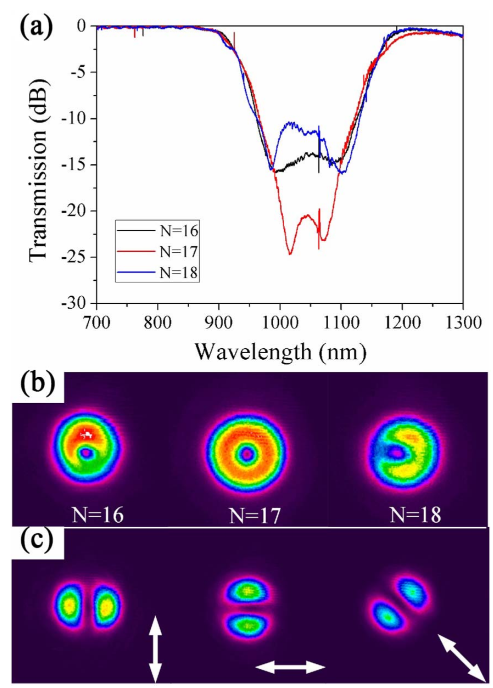

Fig. 5. (a) Transmission spectrum of the LPFG with different grating periods. (b) The mode profile of the LPFG with different periods. (c) The beam profile when the output passes a linear polarizer with different orientations.

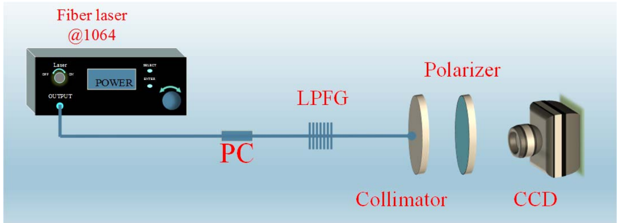

Fig. 6. Schematic of the measurement system.

used to observe the far-field patterns. We find that the best grating period is 17, and a pure LP_{11} mode can be observed by adjusting a polarization controller before the device. As shown in Fig. 5(a), the measured transmission spectra also confirm that the grating period is an important factor for mode conversion efficiency. Figure 5(c) shows the mode distributions after passing through a polarizer, indicating that a TE_{01} mode is generated in the grating.

In conclusion, we have reported an ultra-broadband LPFG-based mode converter at 1 μm inscribed in a TMF by a line-focused continuous-wave CO_2 laser, and the optical properties of the transmission spectrum, output beam profile, and polarization states are investigated numerically and experimentally. By optimizing the grating parameters, the mode conversion efficiency between LP_{01} and LP_{11} modes can reach >99% over the range of 1000 nm to 1085 nm, which covers the main operating band of current high-power fiber lasers. The 3 dB bandwidth is about 240 nm, which is a record value for such devices. This work provides an all-fiber mode converter for high-order fiber lasers, which is helpful for the further power scaling in high-power laser systems.

This work was supported by the Outstanding Youth Science Fund of Natural Science Foundation of Hunan Province (No. 2019JJ20023) and the National Natural Science Foundation of China (No. 11974427).

References

1. R. Ryf, S. Randel, A. H. Gnauck, C. Bolle, A. Sierra, S. Mumtaz, M. Esmaeelpour, E. C. Burrows, R. Essiambre, and P. J. Winzer, J. Lightwave Technol. **30**, 521 (2012).
2. M. Salsi, C. Koebele, D. Sperti, P. Tran, H. Mardoyan, P. Brindel, S. Bigo, A. Boutin, F. Verluise, and P. Sillard, J. Lightwave Technol. **30**, 618 (2012).
3. S. G. Leonsaval, A. Argyros, and J. Blandhawthorn, Photon. Lanterns. Nanophoton. **2**, 429 (2013).
4. A. M. Velazquezbenitez, J. C. Alvarado, J. Lopezgalmiche, J. E. Antoniolopez, J. Sanchezmondragon, P. Sillard, C. M. Okonkwo, and R. Amezcuacorrea, Opt. Lett. **40**, 1663 (2015).
5. S. Wittek, R. R. Bustos, Z. J. Alvarado, E. Z. Sanjabi, J. Bradford, G. G. Lopez, D. Zhang, W. Zhu, J. Antonio-Lopez, and L. Shah, Opt. Lett. **41**, 2157 (2016).
6. T. Mizunami, T. V. Djambova, T. Niiho, and S. Gupta, J. Lightwave Technol. **18**, 230 (2000).
7. C. Wu, Z. Liu, K. M. Chung, M. L. V. Tse, F. Y. M. Chan, A. P. T. Lau, C. Lu, and H. Y. Tam, IEEE Photon. J. **4**, 26 (2012).
8. V. Bhatia and A. M. Vengsarkar, Opt. Lett. **21**, 692 (1996).
9. A. M. Vengsarkar, P. J. Lemaire, J. B. Judkins, V. Bhatia, T. Erdogan, and J. E. Sipe, J. Lightwave Technol. **14**, 58 (1996).
10. A. M. Vengsarkar, J. R. Pedrazzani, J. B. Judkins, P. J. Lemaire, N. S. Bergano, and C. R. Davidson, Opt. Lett. **21**, 336 (1996).
11. S. Ramachandran, Z. Wang, and M. Yan, Opt. Lett. **27**, 698 (2002).
12. M. Yan, S. Ghalmi, S. Ramachandran, and Z. Wang, Opt. Lett. **27**, 1678 (2002).
13. Y. Zhao, Y. Liu, L. Zhang, C. Zhang, J. Wen, and T. Wang, Opt. Express **24**, 6186 (2016).
14. Y. Zhao, Y. Liu, C. Zhang, L. Zhang, G. Zheng, C. Mou, J. Wen, and T. Wang, Opt. Lett. **42**, 4708 (2017).
15. F. Ren, D. Ge, J. Li, Z. Li, Y. He, and Z. Chen, Opt. Commun. **360**, 15 (2016).
16. H. Sakata, H. Sano, and T. Harada, Opt. Fiber Technol. **20**, 224 (2014).
17. Y. Xue, W. Bi, W. Jin, P. Tian, P. Jiang, Q. Liu, and Y. Jin, Optoelectron. Lett. **14**, 81 (2018).
18. Y. Cai, J. Wang, J. Zhang, H. Wan, Z. Zhang, and L. Zhang, Chin. Opt. Lett. **16**, 010602 (2018).
19. J. Xing, J. Wen, J. Wang, F. Pang, Z. Chen, Y. Liu, and T. Wang, Chin. Opt. Lett. **16**, 100604 (2018).
20. S. Ramachandran, J. W. Nicholson, S. Ghalmi, M. F. Yan, P. Wisk, E. Monberg, and F. V. Dimarcello, Opt. Lett. **31**, 1797 (2006).
21. S. Ramachandran, J. M. Fini, M. Mermelstein, J. W. Nicholson, S. Ghalmi, and M. F. Yan, Laser Photon. Rev. **2**, 429 (2010).
22. S. Wang, J. Hu, H. Guo, and X. Zeng, Opt. Express **21**, 3067 (2013).
23. H. Guo, S. Wang, and X. Zeng, IEEE Photon. Technol. Lett. **25**, 1928 (2013).